Asian Journal of Chemistry; Vol. 36, No. 11 (2024), 2666-2674

ASIAN JOURNAL OF CHEMISTRY

https://doi.org/10.14233/ajchem.2024.32700

Synthesis, Characterization, *in Silico* and *in vitro* Screening of Anticancer Activity of Novel Curcumin Analogues

P. SHANMUGASUNDARAM[1,*], D. EASWARAMOORTHY[1], J. HERBERT MABEL[1,*], SRIKANTH JEYABALAN[2] and CHETAN ASHOK[2]

[1]Department of Chemistry, B.S. Abdur Rahman Crescent Institute of Science and Technology, Vandalur-600048, India
[2]Department of Pharmacology, Sri Ramachandra Faculty of Pharmacy, Sri Ramachandra Institute of Higher Education and Research (DU), Porur, Chennai-600116, India

*Corresponding authors: E-mail: pkpshanmugasundaram@gmail.com; herbertjmabel@crescent.education

Received: 12 September 2024; *Accepted*: 24 October 2024; *Published online*: 30 October 2024; AJC-21806

Global problem of cancer associated side effects with current chemotherapeutics and promising anticancer activity of curcumins, intended present study to carry out the synthesis of some new curcumin analogues using chromone aldehydes and cyclic ketones. The study involved *in silico* screening and *in vitro* anticancer evaluation of new synthesized compounds against the breast cancer cell line MDA-MB-231 using the MTT assay. All synthesized compounds exhibited significant cytotoxicity, with IC_{50} values ranging from 34.04 ± 0.05 µg to 43.96 ± 0.05 µg, comparable to the standard drug cisplatin (IC_{50} = 29.25 ± 0.14 µg). Among all new synthesized curcumin analogues, compound **2** exhibited the highest anticancer activity. Molecular docking studies supported these findings, demonstrating strong binding affinities of the chromone compounds to key protein targets EGFR (PDB ID: 3UG2) and ERBB2 (PDB ID: 3H3B), critical in breast cancer pathogenesis. The strong cytotoxic effects and binding affinities suggest that curcumin analogues could serve as promising candidates for developing targeted anticancer therapies.

Keywords: Chromone, Curcumin analogues, Breast cancer, Cytotoxicity, Molecular docking, Targeted therapy.

INTRODUCTION

Benzopyrans (BZPs), a prominent class of small O-heterocycles, play a crucial role in the molecular structure of a diverse array of natural products, pharmaceuticals, biological molecules, agrochemicals and functional materials. They are categorized into six subgroups: coumarins, chromans, 2*H*-chromenes, 4*H*-chromenes, chromones and 4-chromanones. These compounds are widely found in numerous plants and dietary sources, making them a common element in various biological and chemical applications [1]. Chromone, a compound found naturally with a vast array of over 4000 derivatives spread throughout the plant kingdom, ranging from simple algae to complex conifers, is a common component in the diets of both humans and animals. It is distinguished by its lower toxicity levels to mammalian cells [2]. Vegetables often contain chromones in the form of flavone derivatives (2-phenylchromone), flavonol (3-hydroxy-2-phenylchromone) and isoflavone (3-phenylchromone). These flavonoids, which are inherent in chromones, are known for imparting vivid colours to flowers and fruits [1]. Chromones stand out as a pivotal group of heterocycles that underpin a plethora of commercial drugs and biological compounds. The derivatives of chromones are associated with a myriad of pharmacological activities, encompassing antifungal, antibacterial, anti-inflammatory, antioxidant, anticancer, anti-ulcer and anti-HIV properties [2].

The prevalence of cancer is escalating, now recognized as the global second leading cause of mortality, subsequent to cardiovascular diseases [3]. The carcinogenesis process mirrors an evolutionary dynamic, where mutations coupled with natural selection propel uncontrolled proliferation of cells within tissues [4]. Chemotherapy, the frontline therapy for metastatic cancers, employs antineoplastic agents aimed at rapidly dividing cancer cells, yet inadvertently impacts normal fast-growing cells [4]. Such non-selectivity of conventional anticancer drugs leads to toxicities and adverse effects, including bone marrow suppression, alopecia and renal and hepatic injuries, as they also affect healthy cells present in hair follicles, bone marrow and

the gastrointestinal lining [5]. The exploration of natural scaffolds such as curcumins and chromones holds promise in the quest to enhance the specificity of small molecular inhibitors targeting cancer cells. These compounds offer a potential pathway to more selective and less harmful cancer treatments [6,7]. These core structures enable the synthesis of chemical compounds with increased selectivity for cancer cells, effectively targeting and destroying tumor cells. By combining these natural scaffolds with powerful pharmacophores through combinatorial chemistry, it is possible to create targeted therapeutic agents [8].

Curcumin, the primary active ingredient in turmeric, is renowned for its extensive biological activities. Despite its potential, clinical use of curcumin is limited due to its poor bioavailability and rapid metabolism, leading to the need for frequent dosing in therapeutic applications. To overcome these challenges, analogues of curcumin have been synthesized, providing improved bioavailability compared to the original compound [9]. Previously, we reported that curcumin analogues serve as antagonists to combat the hospital acquired infection caused by *Pseudomonas aeruginosa* [10]. Additionally, we also synthesized spirooxindoles from these analogues, which function as anticancer agents [11]. In this research, a series of curcumin analogues featuring a chromone side chain on both ends were meticulously designed with variations in the central ring and substituents on the side chain. These modifications have demonstrated better anticancer properties as compared to standard drug cisplatin.

EXPERIMENTAL

Cyclohexanone, cyclopentanone, dimethylsulfoxide, N-methyl-4-piperidone, 4-oxo-4*H*-chromene-3-carbaldehyde and 6-methyl-4-oxo-4*H*-chromene-3-carbaldehyde were procured from BLD Pharm. F12 medium, DMEM, fetal bovine serum (FBS), penicillin-streptomycin (PenStrep) and trypsin were obtained from Invitrogen, USA. ^{1}H and ^{13}C NMR spectra were recorded using Bruker 400 MHz spectrometer. The chemical shifts (δ) are reported in parts per million (ppm) relative to tetramethylsilane (TMS) as the internal standard. IR spectra were recorded on Shimadzu IR Affinity-1S FTIR spectrometer using KBr pellets. The mass spectra were obtained using a Thermo Scientific Q Exactive mass spectrometer. The mass-to-charge ratio (*m/z*) was recorded, providing the molecular weight of the synthesized compounds.

***In silico* analysis (molecular docking):** Molecular docking studies between ligands and proteins were conducted using Molegro Virtual Docker (MVD) software, chosen for its superior accuracy compared to other docking tools. The ligands were optimized using density functional theory (DFT) with the B3LYP/631G* basis set and subsequently saved in the protein data bank (PDB) format. The target proteins, EGFR and ERBB2, were selected based on a thorough assessment of their resolution and release date from the Protein Data Bank (www.rcsb.org). The chemical structures of the active compounds were retrieved from the PubChem database. In this study, the molecular docking of new curcumin analogues (**1-6**) were carried towards the PDB ID: 3UG2 and 3H3B targets (PDB: 3UG2 is a mutant transferase protein with a resolution of 2.50 Å and represents the epidermal growth factor receptor (EGFR), PDB: 3H3B is a non-mutant immune system protein with a resolution of 2.45 Å and represents the Erb-b2 receptor tyrosine kinase 2 (ERBB2), which are important for cell growth and division). The proteins were prepared in the MVD workspace by removing any excess water molecules and the co-crystallized ligand embedded in the crystal structure. The docking results were determined based on the set scoring functions, such as the MolDock score and Re-rank score [12,13].

General procedure synthesis of new curcumin analogues (1-6): The new curcumin analogues were synthesized based on the standard protocol with minor modifications [10,14,15]. Briefly, a solution containing chromone aldehyde (0.02 M) and cyclic ketone (0.01 M) in 10 mL of ethanol was prepared. Sodium hydroxide (0.01 M) was added under N_2 atmosphere and the mixture was stirred at 65 ºC for 20 min. It was then allowed to cool to room temperature and stirred for another 2 h. The reaction progress was monitored using TLC. After completion of reaction, the mixture was filtered, washed with 5 mL of cold ethanol and dried at 65-70 ºC for 4 h. The crude product was purified by recrystallization from ethanol and dried under reduced pressure to offer pure compound (**Scheme-I**).

3,3′-((1-Methyl-4-oxopiperidine-3,5-diylidene)*bis*(methaneylylidene))*bis*(4*H*-chromen-4-one) (1): Yellow powder, yield: 78 %, m.p.: 185 ºC; IR (KBr, ν_{max}, cm^{-1}): 3095, 2366, 2305, 1639, 1462, 1165 and 760; ^{1}H NMR (300 MHz, $CDCl_3$) δ ppm: 8.29-8.26 (m, Ar-H, 3H), 7.97-7.68 (m, Ar-H, 3H),

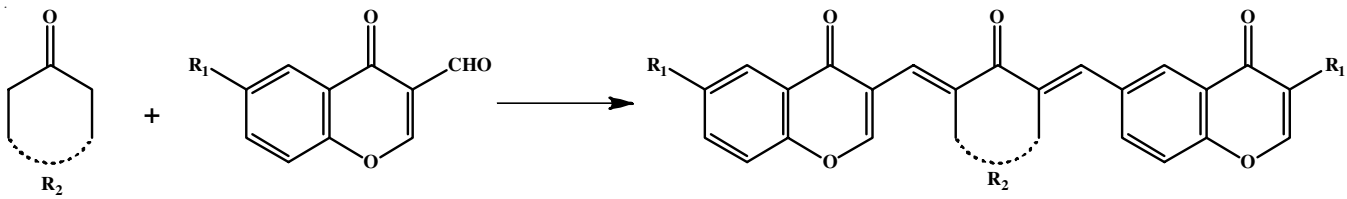

Compound	1	2	3	4	5	6
R_1	—H	—H	—H	—CH_3	—CH_3	—CH_3
R_2	N		—	N		—

Scheme-I: Synthesis of curcumin analogues (**1-6**)

7.50-7.42 (m, Ar-H, 4H), 3.63 (m, -CH_2, 4H) and 2.43 (N-CH_3, 3H); Mass (*m/z*): 426 [M+1].

3,3′((2-Oxocyclohexane-1,3-diylidene)*bis*(methaneylylidene))*bis*(4*H*-chromen-4-one) (2): Yellow powder, yield: 81%, m.p.: 176 ºC; IR (KBr, ν_{max}, cm^{-1}): 3088, 2916, 1693, 1608, 1461, 1140, 1214 and 755; ^{1}H NMR (300 MHz, DMSO-d_6) δ ppm: 8.79 (m, Ar-H, 2H), 8.16-8.13 (m, Ar-H, 2H), 7.89-7.84 (m, Ar-H, 2H), 7.75-7.72 (m, Ar-H, 2H), 7.58-7.53 (m, Ar-H, 4H), 3.02 (m, -CH_2-, 4H) and 1.23 (m, -CH_2-, 2H), ^{13}C NMR (75 MHz, DMSO-d_6) δ ppm: 175.49, 155.96, 155.81, 134.06, 123.41, 125.76, 120.49, 118.13, 57.15 and 22.69; Mass (*m/z*): 411 [M+1].

3,3′-((2-Oxocyclopentane-1,3-diylidene)*bis*(methaneylylidene))*bis*(4*H*-chromen-4-one) (3): Yellow powder, yield: 64%, m.p.: 178 ºC; IR (KBr, ν_{max}, cm^{-1}): 3084, 2909, 1664, 1608, 1463, 1138, 1221 and 762; ^{1}H NMR (300 MHz, $CDCl_3$) δ ppm: 8.79 (m, Ar-H, 2H), 8.28-8.22 (m, Ar-H, 2H), 8.00 (m, Ar-H, 2H), 7.72-7.67 (m, Ar-H, 4H), 7.48-7.40 (m, Ar-H, 4H), 2.79-2.75 (m, -CH_2-, 4H); Mass (*m/z*): 397 [M+1].

3,3′-((1-Methyl-4-oxopiperidine-3,5-diylidene)*bis*-methaneylylidene))*bis*(4*H*-chromen-4-one) (4): Yellow powder, Yield: 73%, m.p.: 190 ºC; IR (KBr, ν_{max}, cm^{-1}): 3027, 2909, 2835, 2756, 2343, 1646, 1481, 1200 and 806: ^{1}H NMR (300 MHz, $CDCl_3$) δ ppm: 8.05 (m, Ar-H, 2H), 7.94 (m, Ar-H, 2H), 7.74 (m, Ar-H, 2H), 7.52-7.49 (m, Ar-H, 2H), 7.39-7.36 (m, 2H), 3.62 (m, -CH_2-, 4H), 2.471 (m, CH_3, 6H), 2.426 (m, N-CH_3, 3H); Mass (*m/z*): 454 [M+1].

3,3′-((2-Oxocyclohexane-1,3-diylidene)*bis*(methaneylylidene))*bis*(6-methyl-4*H*-chromen-4-one) (5): Yellow powder, yield: 84%, m.p.: 192 ºC; IR (KBr, ν_{max}, cm^{-1}): 3024, 2920, 1602, 1482 1200 and 768: ^{1}H NMR (300 MHz, DMSO-d_6) δ ppm: 8.75 (m, Ar-H, 2H), 7.94 (m, Ar-H, 2H), 7.70-7.62 (m, Ar-H, 4H), 7.55 (m, Ar-H, 2H), 3.00 & 1.23 (-CH_2-, 6H: Ar-CH_3, 6H): Mass (*m/z*): 439 [M+1].

3,3′-((2-Oxocyclopentane-1,3-diylidene)*bis*(methaneylylidene))*bis*(6-methyl-4*H*-chromen-4-one) (6): Yellow powder, yield: 69%, m.p.: 188 ºC; IR (KBr, ν_{max}, cm^{-1}): 3095, 2949, 2903, 2845, 1640, 1481, 1131, 799 and 768: ^{1}H NMR (300 MHz, $CDCl_3$) δ ppm: 8.04 (m, Ar-H, 2H), 7.98 (m, Ar-H, 2H), 7.70 (m, Ar-H, 2H), 7.51-7.48 (m, Ar-H, 2H), 7.38-7.35 (m, Ar-H, 2H), 2.78-2.75 (m, -CH_2-, 4H) and 1.23 (m, Ar-CH_3, 6H): Mass (*m/z*): 425 [M+1].

***In vitro* anticancer activity (MTT assay):** The new curcumin analogues were further evaluated for their anticancer potential (against MDA-MB-231) using standard MTT assay with minor modifications [11]. The MDA-MB-231 cell lines were procured from ATCC and subjected to cell culturing using standard protocol [16]. In brief, stock cells were cultured in DMEM/F12 medium supplemented with 10% inactivated Fetal Bovine Serum (FBS), 100 IU/mL penicillin and 100 µg/mL streptomycin and maintained in a humidified atmosphere of 5% CO_2 at 37 ºC until confluence was reached. Cells were then dissociated using a solution containing 0.2% trypsin, 0.02% EDTA and 0.05% glucose in PBS. After checking cell viability, the cells were centrifuged. Subsequently, 50,000 cells per well were plated in a 96-well plate and incubated for 24 h at 37 ºC in a 5% CO_2 incubator.

The monolayer cell culture was trypsinized and the cell concentration was adjusted to 1.0×10^5 cells/mL using media containing 10% FBS. A total of 100 µL of diluted cell suspension (50,000 cells/well) was added to each well of a 96-well microtiter plate. After 24 h, when a partial monolayer had formed, the supernatant was removed, the monolayer was washed with fresh medium and 100 µL of varying concentrations of chromone and cisplatin (0, 10, 20, 30, 40, 50, 60, 70, 80, 90 and 100 µg/mL) were added to the wells. The plates were incubated at 37 ºC for 24 h in a 5% CO_2 atmosphere. After incubation, the test solutions were discarded and 100 µL of MTT solution (5 mg/10 mL in PBS) was added to each well. The plates were then incubated for an additional 4 h at 37 ºC in a 5% CO_2 atmosphere. Following this, the supernatant was removed and 100 µL of DMSO was added to each well. The plates were gently shaken to dissolve the formazan crystals. Absorbance was measured using a microplate reader at 590 nm. The percentage of growth inhibition was calculated using the following formula and the IC_{50} values (the concentration required to inhibit cell growth by 50%) were determined from the dose-response curves for each cell line [17,18]:

$$\text{Inhibition } (\%) = 100 - \frac{\text{OD of sample}}{\text{OD of control}} \times 100$$

Statistical analysis: The statistical methods used to analyze the data and derive the IC_{50} values, which represent the concentration of the compound that inhibits 50% of the cell growth. The IC_{50} values were obtained by fitting a sigmoid dose-response curve to the data using a nonlinear regression analysis. The software used for the analysis was Graph Pad Prism 6.34 [19].

Target prediction of chromone against breast cancer: The potential targets of chromones were identified using the Swiss Target Prediction database. Canonical SMILES were retrieved from the PubChem database and uploaded to the Swiss Target Prediction server [20]. The species "Homo sapiens" was selected to convert UniProt IDs to gene symbols. Concurrently, the breast cancer targets were identified using the GeneCards database by searching for the keyword "breast cancer" to collect potential genes [21,22]. Further analysis involved overlapping the breast cancer targets and chromone targets using a Venn diagram to represent the potential targets of chromones against breast cancer.

Gene ontology and KEGG pathway enrichment analysis: The core mechanisms and pathways underlying the antibreast cancer effects of the synthesized chromones were explored through Gene Ontology (GO) functional analysis and KEGG pathway enrichment. Hub genes identified from the overlaps were analyzed using the DAVID database, with the species restricted to Homo sapiens. Data were gathered on biological processes (BP), cellular components (CC), molecular functions (MF) and KEGG pathways [22].

Construction of compound target network: Cytoscape 3.10.0 was used to construct and visualize biomolecular interaction networks, serving as a powerful tool for comprehensive analysis. In the network diagrams generated, each node represented either an active constituent or a target gene, while the edges between the nodes depicted the interactions between

the active constituents and their respective target genes. This visualization allowed for a clear representation of the complex relationships and interactions within the network. Cytoscape aids in effective analysis and interpretation of the intricate web of interactions, facilitating a deeper understanding of the underlying mechanisms of the synthesized chromones' antibreast cancer effects [23].

Protein protein interaction (PPI) network construction: The STRING database (version 12) was used to construct a protein-protein interaction (PPI) network to investigate the functional interactions related to chromone's anti-breast cancer effects. A network confidence score of ≥ 0.4 was applied to identify relevant targets, with "Homo sapiens" selected in Cytoscape software (version 3.10.2). The CytoHubba plug-in was then utilized to identify key targets associated with chromone's antibreast cancer activity. The most significant targets were analyzed using the CytoHubba plug-in in Cytoscape, selecting the top 10 Hubba nodes based on the Maximal Clique Centrality (MCC) ratio [24].

RESULTS AND DISCUSSION

The associated side effects with available chemotherapeutics and the high biological potential of curcumin moiety, emphasizes the need for design, synthesis and anticancer evaluation of new curcumin analogues [17]. Present study offered substituted cycloalkyl-1,3-diylidene-*bis*(methaneylylidene)-*bis*(susbtituted-4*H*-chromen-4-one) analogues (**1-6**), by undergoing enolization, followed by condensation and dehydration. The synthesis of new curcumin analogues involved the reaction of chromone aldehyde with cyclic ketones under basic conditions. The dehydration step is facilitated by the formation of a stable conjugated system in the product, which is thermodynamically favourable [25]. The purification of synthesized new curcumin analogues was done through recrystallization of all crudes with ethanol and activated charcoal. The structures of the newly synthesized curcumin analogues were confirmed based on their FTIR, ^{1}H NMR, ^{13}C NMR and mass spectrometric data and supported by literature [26,27]. The presence of characteristic FTIR bands at 3024-3095 cm^{-1} for =C-H stretching, ^{1}H NMR signal at δ 3.63-2.75 (m, -CH_2) and the characteristic M+1 peak corresponding to their molecular weight in the respective mass spectra confirmed the structure of new curcumin analogues (**1-6**).

Screening of chromone targets and breast cancer disease targets: A total of 196 targets for curcumin analogues were identified. Additionally, 1,748 breast cancer-related targets were sourced from the Genecards database. Duplicate targets found in both the curcumin analogues and disease target files were removed, leaving only unique entries. The remaining targets for chromones and breast cancer were analyzed using Venn Diagram 2.1.0, revealing 72 overlapping genes that are potential targets for chromone's antibreast cancer activity.

These targets were involved in various critical biological pathways, such as the PI3K-Akt signalling pathway, MAPK signalling pathway and pathways in cancer. Gene ontology and KEGG pathway enrichment analyses highlighted the involvement of curcumin analogues in key biological processes like phosphorylation, signal transduction and positive regulation of cell proliferation. These pathways are known to be pivotal in cancer progression and metastasis, suggesting that curcumin analogues may exert their anticancer effects by modulating these essential biological functions [28,29].

Compound target network analysis: Curcumin analogues were selected alongside 196 targets and their associated pathways, which included the highest number of genes. This strategy was used to create a network diagram in cytoscape, illustrating the relationships between active compounds, target genes and pathways. The presence of multiple targets for each compound suggests their potential as therapeutic agents for breast cancer, possibly enhancing efficacy by simultaneously affecting various targets. The network analysis of hub genes is presented in Fig. 1, while the network construction is shown in Fig. 2.

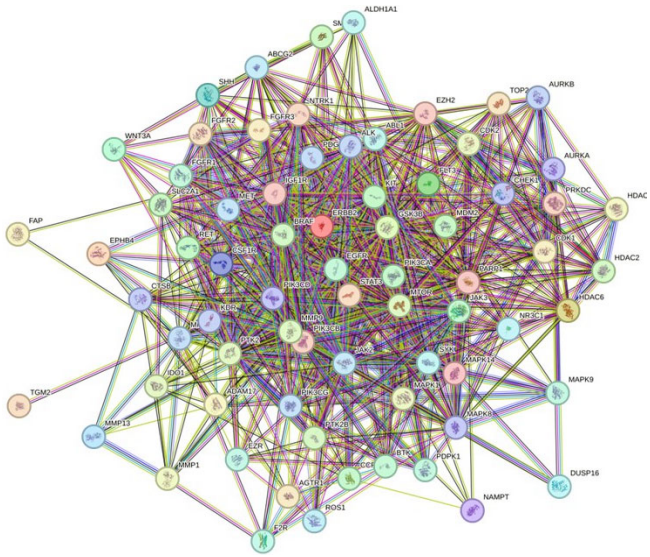

Fig. 1. Network analysis of the hub-genes from Venny 2.1.0.

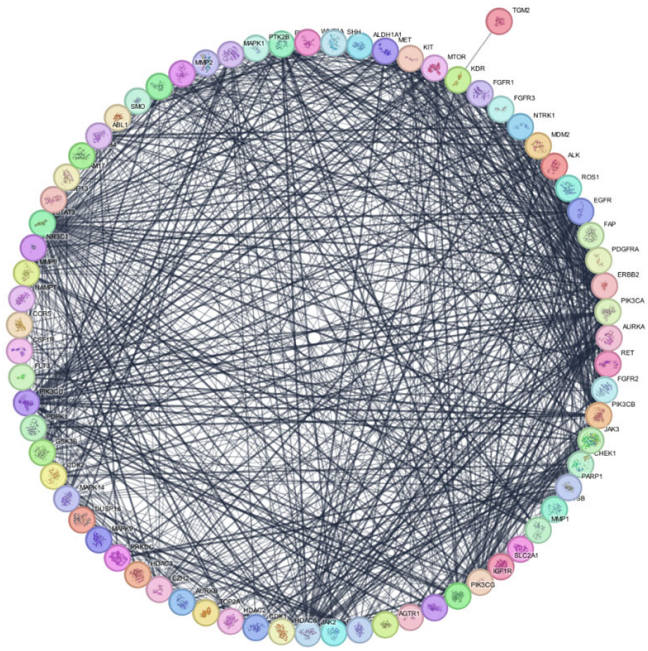

Fig. 2. Network construction of hub-genes

Gene ontology function and KEGG pathway enrichment analysis: From the DAVID database, we obtained a total of 578 Gene Ontology (GO) items, including 438 biological process (BP) items, 65 cellular component (CC) items and 75 molecular function (MF) items. The top 10 items from each category were selected for visualization based on p-values (less than 0.05) and highest counts. The histogram displays the degree of enrichment on the ordinary axis. The BP functions of chromones in breast cancer primarily involve phosphorylation, protein phosphorylation, signal transduction, positive regulation of cell proliferation, negative regulation of apoptosis, protein autophosphorylation, positive regulation of PI3K/AKT signalling, multicellular organism development, positive regulation of cell migration and positive regulation of gene expression. The MF items mainly include plasma membrane, cytosol, cytoplasm, nucleus, membrane, nucleoplasm, receptor complex, extracellular region, cell surface and protein-containing complex. These GO functions support the potential use of curcumin analogues in breast cancer treatment. KEGG pathway enrichment analysis revealed that chromones were involved in 137 signalling pathways. The top 10 enriched pathways were visualized using a bubble chart, where bubble size and p-values indicate the extent of enrichment. Key pathways included MicroRNAs in cancer, MAPK signalling, PI3K-Akt signalling, Ras signalling, pathways and proteoglycans in cancer, endocrine resistance, prostate cancer, EGFR tyrosine kinase inhibitor resistance and central carbon metabolism in cancer. Figs. 3 and 4 illustrate the biological process, cellular component and molecular function pathways of the hub genes and the KEGG pathways for top hub gene targets, respectively.

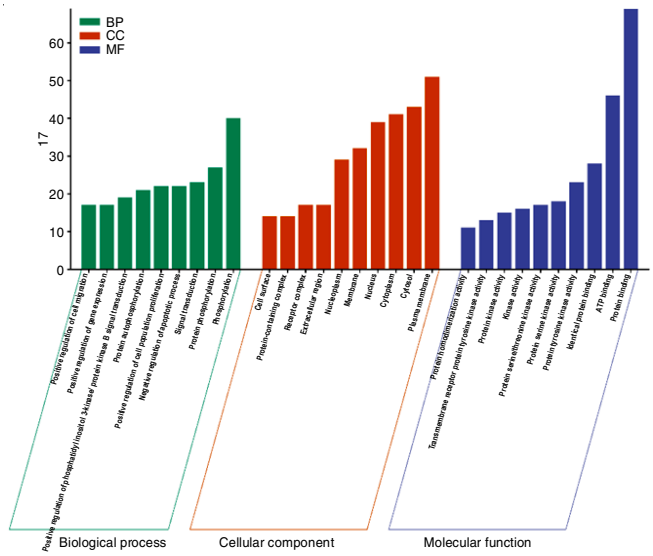

Fig. 3. Biological process, cellular component, molecular function pathways of the hub-genes

Protein-protein interaction (PPI) network analysis: A total of 72 hub genes were submitted to the STRING database for protein-protein interaction (PPI) network analysis. Cytoscape software was subsequently used to visualize and analyze the network, evaluating the degree of each gene, where higher degrees signify more prominent roles within the network. The

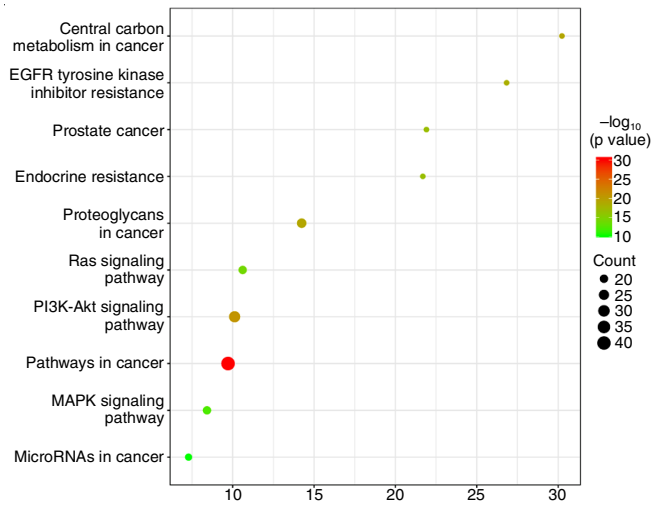

Fig. 4. The KEGG pathway of the top targets of hub-genes

CytoHubba plug-in was also employed to identify key targets. The top 10 core targets identified were EGFR, ERBB2, IGF1R, JAK2, PIK3CA, STAT3, PIK3CB, MET, MTOR and KDR. Fig. 5 shows the network analysis of these top-ranked targets. The high degree of interaction among these proteins indicates that curcumin analogues could potentially disrupt multiple signalling pathways simultaneously, enhancing their efficacy as anticancer agents. This multi-target approach is advantageous in cancer therapy as it can overcome the limitations of single target treatments and reduce the likelihood of drug resistance [30,31].

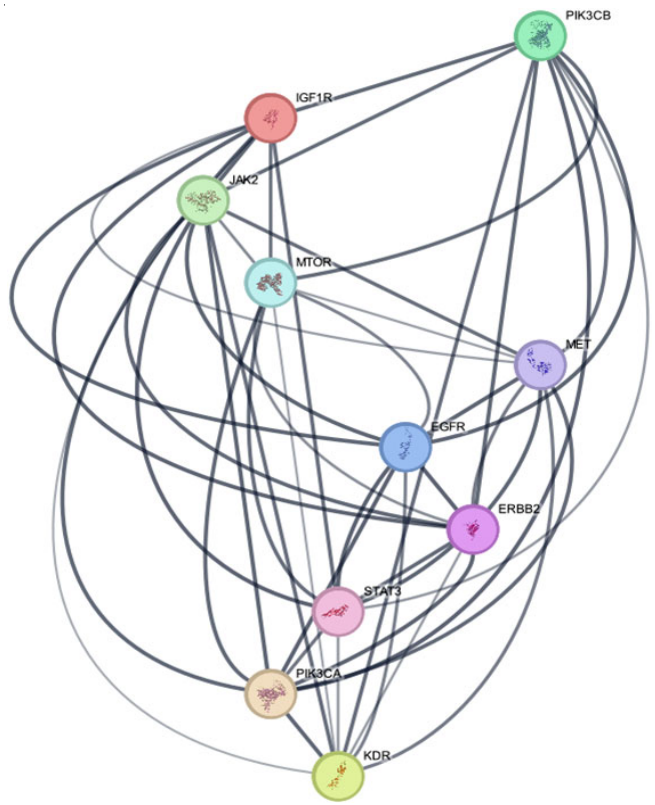

Fig. 5. Network analysis of top-ranked targets (red colour indicates top order - highly interactive; orange colour indicates - moderate interactive; yellow colour indicates -mild interactive)

Molecular docking studies: The molecular docking analysis was performed for the curcumin analogues towards PDB: 3UG2 and 3H3B. The binding affinity of all the curcumin analogues ranged from -185 to -104 MolDock score. Among the curcumin analogues, compounds **4** and **6** exhibited the highest MolDock score. Compound **6** exhibited a score of -124.904 against EGFR and -179.816 against ERBB2, while compound **4** exhibited a score of -113.687 against EGFR and -185.33 towards ERBB2, exhibiting their potential to bind the target proteins of breast cancer. These findings align with previous research that emphasizes the importance of EGFR and ERBB2 as therapeutic targets in breast cancer treatment [32,33]. The molecular docking score of curcumin analogues is given in Table-1. The docking images of curcumin analogues is illustrated in Figs. 6 and 7.

TABLE-1
MOLECULAR DOCKING REPORT OF CURCUMIN ANALOGUES TOWARDS EGFR AND ERBB2

Compound	Molecular docking scores (kcal/mol)	
	EGFR (PDB ID: 3UG2)	ERBB2 (PDB ID: 3H3B)
1	-107.264	-169.452
2	-107.159	-158.711
3	-104.915	-170.658
4	-113.687	-185.33
5	-112.674	-142.034
6	-124.904	-179.816

Curcumin analogues inhibited MDA-MB-231: To confirm the effects of curcumin analogues on MDA-MB-231 cells, as suggested by the network pharmacology analysis, an MTT assay

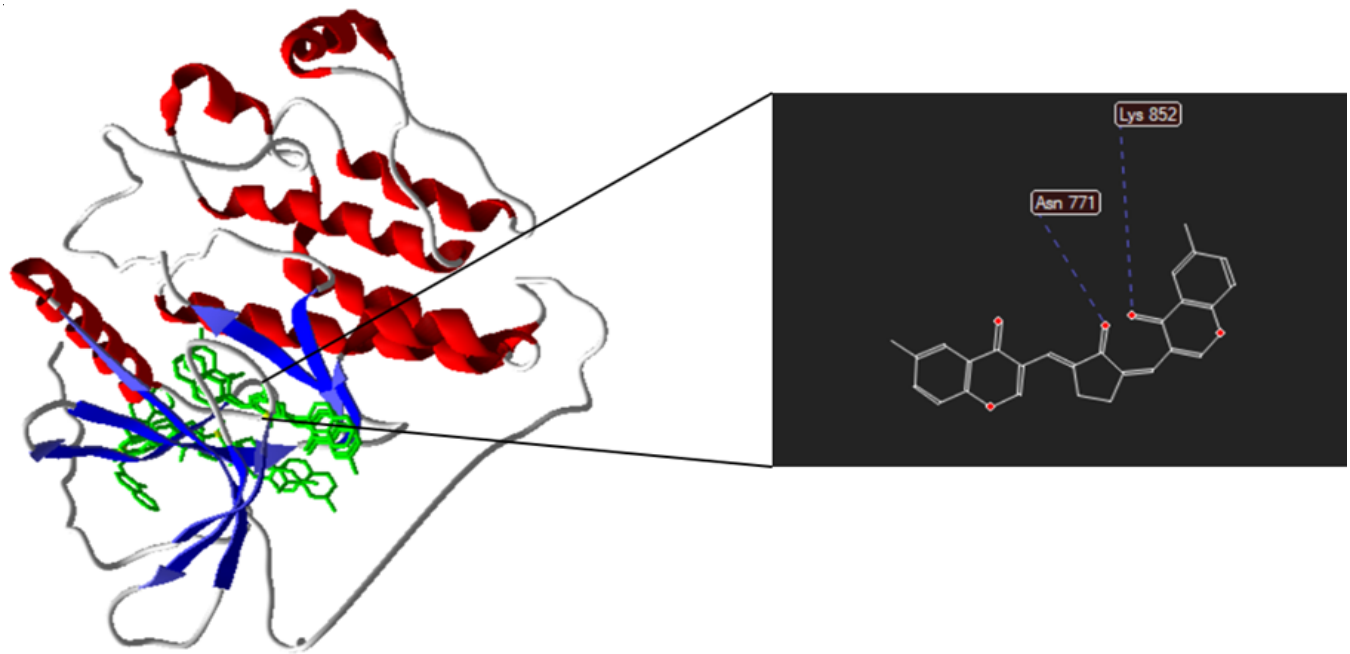

Fig. 6. Molecular docking image of curcumin analogues compound 6 against EGFR proteins

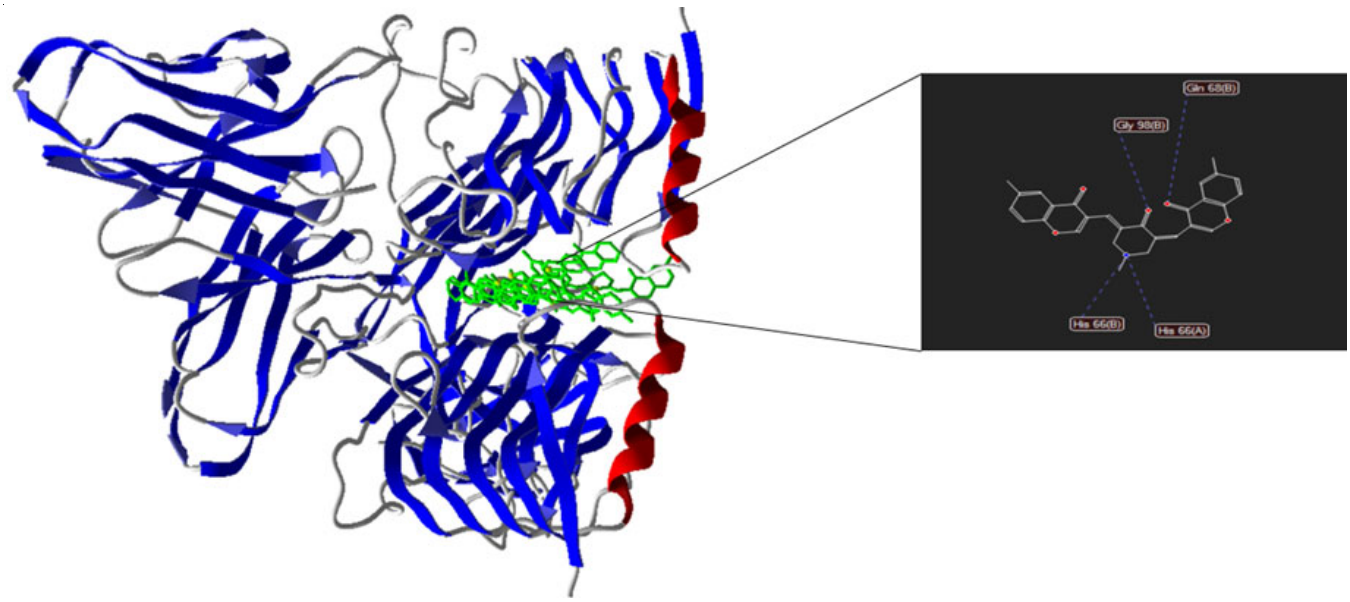

Fig. 7. Molecular docking image of curcumin analogues compound **4** against ERBB2 protein

was performed. This assay assessed the impact of curcumin analogues on cell viability in MDA-MB-231 cells. Following a 48 h exposure to curcumin analogues at concentrations ranging from 0 to 100 µg/mL, a dose-dependent reduction in cell viability was observed (Figs. 8 and 9). The IC_{50} values for the curcumin analogues varied between 34.04 and 43.96 µg/mL in MDA-MB-231 cells. Cisplatin, used as a reference drug, exhibited an IC_{50} of 29.25 µg/mL. These results indicate varying levels of potency among the compounds, with cisplatin showing the lowest IC_{50} and thus the highest efficacy in comparison. The IC_{50} values of curcumin analogues and cisplatin is given in Table-2. Among the synthesized compounds, Compound **2** exhibited the highest potency, making it a promising candidate for further development as a targeted anticancer agent.

Supplementary materials: Supplementary data related to hub-genes among these overlapping targets (for screening of chromone targets and breast cancer disease targets); Biological pathways, cellular components, molecular functions and KEGG pathways (for gene ontology function and KEGG pathway enrichment analysis); and the top targets (for protein-protein interaction network analysis) will be provided by the authors on request.

TABLE-2
HALF-MAXIMAL INHIBITORY CONCENTRATION OF COMPOUNDS

Compound	IC_{50} (µg/mL)
1	41.82
2	34.04
3	43.96
4	41.51
5	40.20
6	41.11
Cisplatin	29.25

Conclusion

In this study, few curcumin analogues were synthesized, characterized and evaluated for their anticancer potential against MDA-MB-231 breast cancer cells. The study offered successful synthesis of new curcumin analogues. The synthesized compounds demonstrated significant cytotoxicity, with IC_{50} values comparable to cisplatin, standard reference drug. Compound **2** showed the highest potency, whreas the molecular docking revealed strong binding affinities to EGFR and ERBB2, critical targets in breast cancer. Network pharmacology identified key

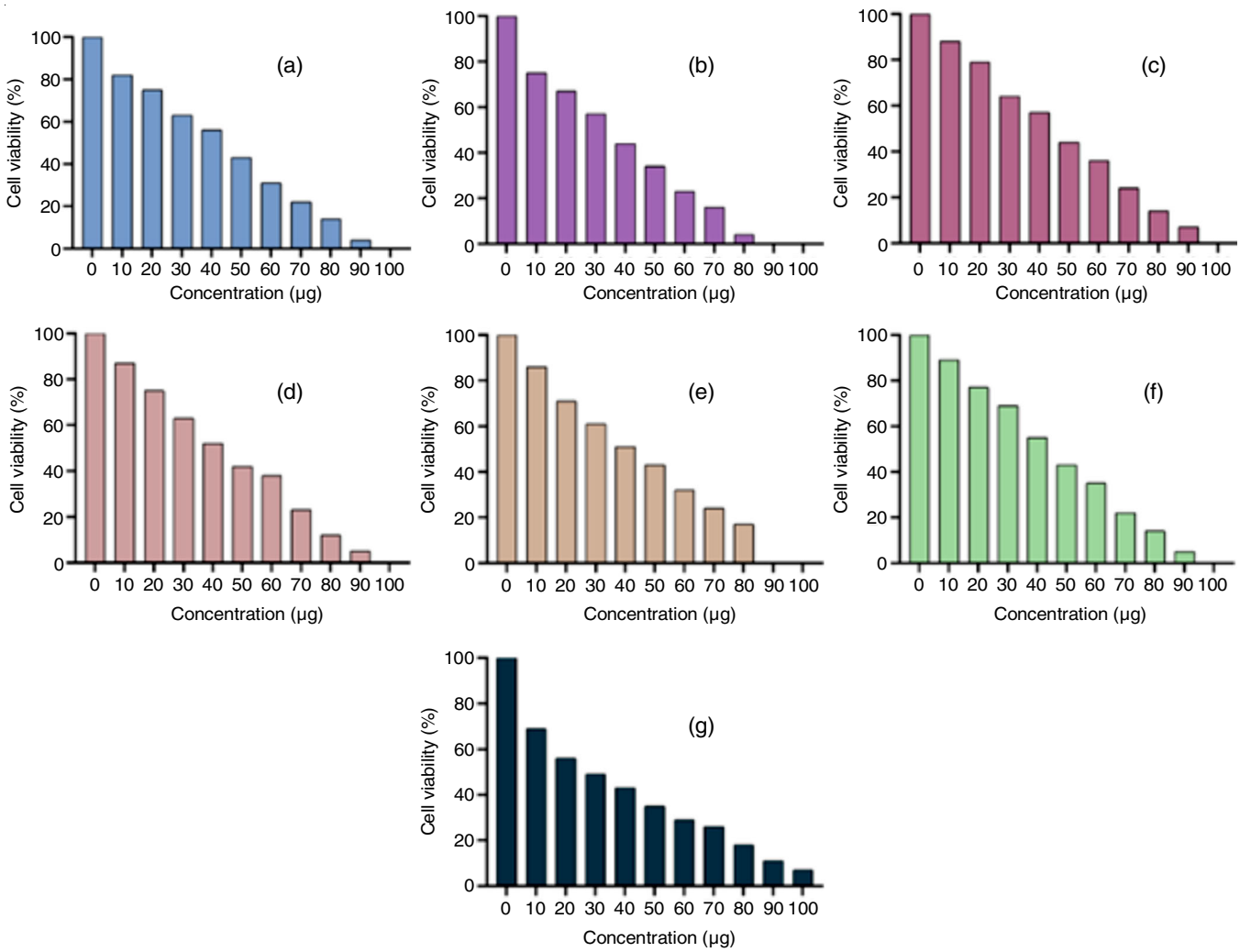

Fig. 8. Cell viability of MDA-MB-231 cells at different concentration of the test drugs, (a) compound **1**, (b) compound **2**, (c) compound **3**, (d) compound **4**, (e) compound **5**, (f) compound **6**, (g) cisplatin (reference drug)

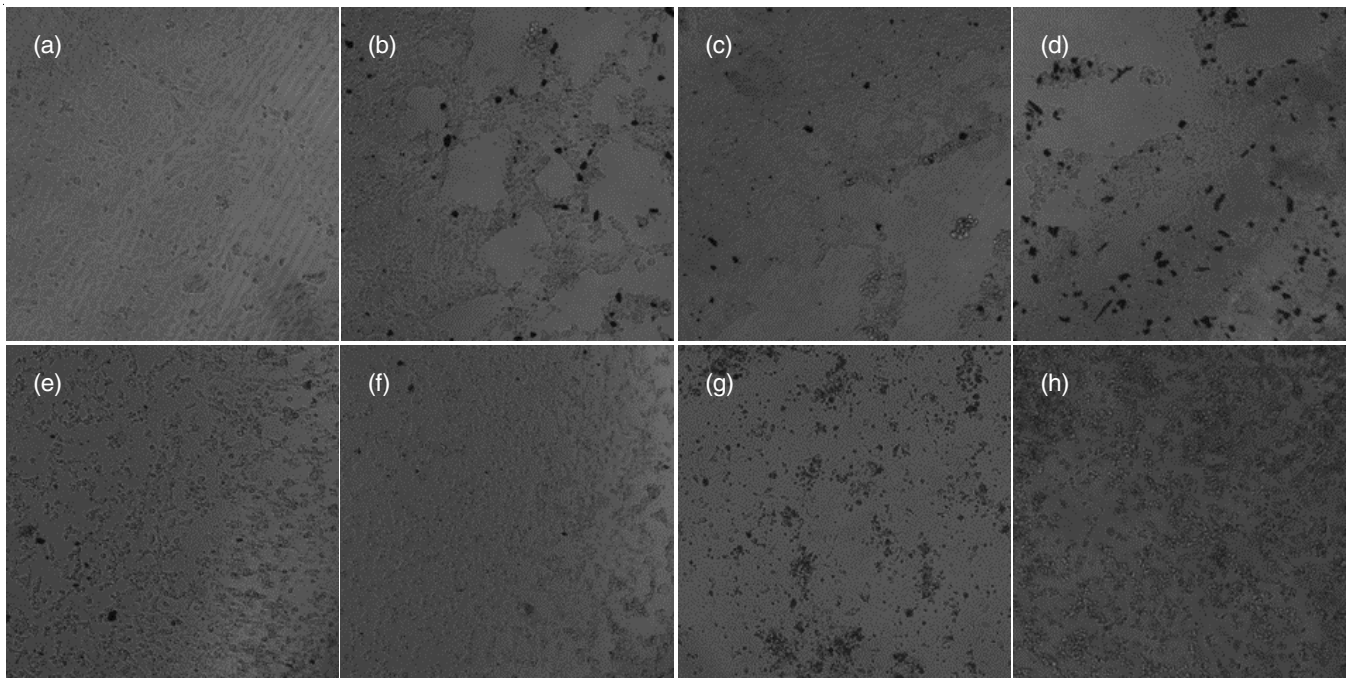

Fig. 9. Transwell invasion abilities of MDA-MB-231 cells in the presence of chromones and cisplatin (n = 3); (a) control, (b) compound **1**, (c) compound **2**, (d) compound **3**, (e) compound **4**, (f) compound **5**, (g) compound **6** and (h) cisplatin (reference drug)

pathways and targets involved in the anticancer effects of curcumin analogues. These findings highlight the potential of curcumin analogues as targeted anticancer agents, warranting further investigation and development for breast cancer therapy.

ACKNOWLEDGEMENTS

Authors are thankful to B.S. Abdur Rahman Crescent Institute of Science and Technology, Vandalur, India for the support to successfully completion of this study.

CONFLICT OF INTEREST

The authors declare that there is no conflict of interests regarding the publication of this article.

REFERENCES

1. E. Middleton, C. Kandaswami and T.C. Theoharides, *Pharmacol. Rev.*, **52**, 673 (2000).
2. M.-H. Pan and C.-T. Ho, *Chem. Soc. Rev.*, **37**, 2558 (2008); https://doi.org/10.1039/b801558a
3. F. Bray, M. Laversanne, H. Sung, J. Ferlay, R.L. Siegel, I. Soerjomataram and A. Jemal, *CA Cancer J. Clin.*, **74**, 229 (2024); https://doi.org/10.3322/caac.21834
4. M.M. Gottesman, O. Lavi, M.D. Hall and J.-P. Gillet, *Annu. Rev. Pharmacol. Toxicol.*, **56**, 85 (2016); https://doi.org/10.1146/annurev-pharmtox-010715-103111
5. D. Hanahan and R.A. Weinberg, *Cell*, **144**, 646 (2011); https://doi.org/10.1016/j.cell.2011.02.013
6. D.J. Newman and G.M. Cragg, *J. Nat. Prod.*, **79**, 629 (2016); https://doi.org/10.1021/acs.jnatprod.5b01055
7. D.K. Agrawal and P.K. Mishra, *Med. Res. Rev.*, **30**, 818 (2010); https://doi.org/10.1002/med.20188
8. M.-J.R. Howes, N.S.L. Perry and P.J. Houghton, *Phytother. Res.*, **17**, 1 (2003); https://doi.org/10.1002/ptr.1280
9. A. Goel, A.B. Kunnumakkara and B.B. Aggarwal, *Biochem. Pharmacol.*, **75**, 787 (2008); https://doi.org/10.1016/j.bcp.2007.08.016
10. P. Shanmugasundaram, S.S. Kumar, R. Ubaid, D. Easwaramoorthy, S.M. Gowri and S. Hemalatha, *Biocatal. Agric. Biotechnol.*, **20**, 101238 (2019); https://doi.org/10.1016/j.bcab.2019.101238
11. P. Shanmugasundaram, D. Easwaramoorthy, A.R. Mhashal and A. Khan, *Rasayan J. Chem.*, **16**, 1599 (2023); https://doi.org/10.31788/RJC.2023.1638506
12. S.H. Abdullahi, A. Uzairu, G.A. Shallangwa, S. Uba and A.B. Umar, *J. Egypt. Natl. Canc. Inst.*, **35**, 24 (2023); https://doi.org/10.1186/s43046-023-00182-3
13. G. Bitencourt-Ferreira and W.F. de Azevedo, in eds.: W.F. de Azevedo Jr., Molegro Virtual Docker for Docking. In: Docking Screens for Drug Discovery, New York, NY: Springer; pp. 149–167 (2019).
14. C. Demetgül and N. Beyazit, *Carbohydr. Polym.*, **181**, 812 (2018); https://doi.org/10.1016/j.carbpol.2017.11.074
15. C.M.M. Santos, V.L.M. Silva and A.M.S. Silva, *Molecules*, **22**, 1665 (2017); https://doi.org/10.3390/molecules22101665
16. S. Monika and R. Ramesh, *New J. Chem.*, **47**, 15622 (2023); https://doi.org/10.1039/D3NJ02869K
17. M. Ghasemi, T. Turnbull, S. Sebastian and I. Kempson, *Int. J. Mol. Sci.*, **22**, 12827 (2021); https://doi.org/10.3390/ijms222312827
18. T. Ibrahim, L. Mercatali, E. Sacanna, A. Tesei, S. Carloni, P. Ulivi, C. Liverani, F. Fabbri, M. Zanoni, W. Zoli and D. Amadori, *Cancer Cell Int.*, **12**, 48 (2012); https://doi.org/10.1186/1475-2867-12-48
19. M. Marinovic, H. Rimac, L.P. de Carvalho, C. Rôla, S. Santana, K. Pavic, J. Held, M. Prudêncio and Z. Rajic, *Bioorg. Med. Chem.*, **94**, 117468 (2023); https://doi.org/10.1016/j.bmc.2023.117468
20. A. Daina, O. Michielin and V. Zoete, *J. Chem. Inf. Model.*, **54**, 3284 (2014); https://doi.org/10.1021/ci500467k
21. F. Lin, G. Zhang, X. Yang, M. Wang, R. Wang, M. Wan, J. Wang, B. Wu, T. Yan and Y. Jia, *J. Ethnopharmacol.*, **303**, 115933 (2023); https://doi.org/10.1016/j.jep.2022.115933
22. L. Lv, J. Du, D. Wang and Z. Yan, *Drug Des. Devel. Ther.*, **18**, 375 (2024); https://doi.org/10.2147/DDDT.S441126
23. P. Shannon, A. Markiel, O. Ozier, N.S. Baliga, J.T. Wang, D. Ramage, N. Amin, B. Schwikowski and T. Ideker, *Genome Res.*, **13**, 2498 (2003); https://doi.org/10.1101/gr.1239303
24. S. Sabarathinam, *Sci. Rep.*, **14**, 14852 (2024); https://doi.org/10.1038/s41598-024-61779-9

25. M.B. Smith, March's Advanced Organic Chemistry: Reactions, Mechanisms and Structure, John Wiley & Sons (2020).
26. M. Kanehisa, M. Furumichi, M. Tanabe, Y. Sato and K. Morishima, *Nucleic Acids Res.*, **45(D1)**, D353 (2017); https://doi.org/10.1093/nar/gkw1092
27. M. Ashburner, C.A. Ball, J.A. Blake, D. Botstein, H. Butler, J.M. Cherry, A.P. Davis, K. Dolinski, S.S. Dwight, J.T. Eppig, M.A. Harris, D.P. Hill, L. Issel-Tarver, A. Kasarskis, S. Lewis, J.C. Matese, J.E. Richardson, M. Ringwald, G.M. Rubin and G. Sherlock, *Nat. Genet.*, **25**, 25 (2000); https://doi.org/10.1038/75556
28. N.K. Fuloria and S. Fuloria, *J. Anal. Bioanal. Technol.*, **s11**, 1 (2013); https://doi.org/10.4172/2155-9872.S11-001
29. S. Fuloria, Spectroscopy: Fundamental and Data Interpretation, Studium Press (2013).
30. A.-L. Barabási, N. Gulbahce and J. Loscalzo, *Nat. Rev. Genet.*, **12**, 56 (2011); https://doi.org/10.1038/nrg2918
31. J. Barretina, G. Caponigro, N. Stransky, K. Venkatesan, A.A. Margolin, S. Kim, C.J. Wilson, J. Lehár, G.V. Kryukov, D. Sonkin, A. Reddy, M. Liu, L. Murray, M.F. Berger, J.E. Monahan, P. Morais, J. Meltzer, A. Korejwa, J. Jané-Valbuena, F.A. Mapa, J. Thibault, E. Bric-Furlong, P. Raman, A. Shipway, I.H. Engels, J. Cheng, G.K. Yu, J. Yu, P. Aspesi, M. de Silva, K. Jagtap, M.D. Jones, L. Wang, E. Palescandolo, S. Gupta, M. Reich, C. Hatton, S. Mahan, C. Sougnez, R.C. Onofrio, T. Liefeld, L. MacConaill, W. Winckler, N. Li, J.P. Mesirov, S.B. Gabriel, G. Getz, K. Ardlie, V. Chan, V.E. Myer, B.L. Weber, J. Porter, M. Warmuth, P. Finan, J.L. Harris, M. Meyerson, T.R. Golub, M.P. Morrissey, W.R. Sellers, R. Schlegel and L.A. Garraway, *Nature*, **483**, 603 (2012); https://doi.org/10.1038/nature11003
32. S.M. Swain, M. Shastry and E. Hamilton, *Nat. Rev. Drug Discov.*, **22**, 101 (2023); https://doi.org/10.1038/s41573-022-00579-0
33. N. O'Donovan and J. Crown, *Anticancer Res.*, **27**, 1285 (2007).